

Selection of the optimal electrochemical machining process parameters using biogeography-based optimization algorithm

Rajarshi Mukherjee · Shankar Chakraborty

Received: 5 March 2011 / Accepted: 12 March 2012 / Published online: 29 March 2012
© Springer-Verlag London Limited 2012

Abstract Electrochemical machining (ECM) has become one of the most potential and useful non-traditional machining processes because of its capability of machining complex and intricate shapes in high-strength and heat-resistant materials. For effective utilization of the ECM process, it is often required to set its different machining parameters at their optimal levels. Various mathematical techniques have already been proposed by past researchers to determine the optimal combinations of the different machining parameters of the ECM process. In this paper, the machining parameters of an ECM process and a wire electrochemical turning process are optimized using the biogeography-based optimization (BBO) algorithm. Both the single- and multi-response optimization models are considered. The optimization performance of the BBO algorithm is also compared with that of other population-based algorithms, e.g., genetic algorithm and artificial bee colony algorithm. It is observed that the BBO algorithm outperforms the others with respect to the optimal values of different process responses and computation time.

Keywords Electrochemical machining · Wire electrochemical turning · Process parameter · Response · Biogeography-based optimization · Algorithm

1 Introduction

Electrochemical machining (ECM) was introduced in the late 1950s and early 1960s in defense and aerospace

industries and has now been extended to many other industries, such as automotive, forging dies, electrical and surgical components [1–4], and, recently, in miniature manufacturing [5]. Nowadays, ECM has become one of the most useful and potential non-traditional machining processes applied to a variety of machining operations, e.g., turning, drilling, grinding, deburring, and cavity sinking. It also provides an economical and effective method for machining high-strength, heat-resistant materials into complex and intricate shapes which are difficult to be machined using the conventional metal machining techniques. The material removal mechanism of the ECM process is based on electrolysis where metals are liberated from the workpiece surface atom by atom. In an electrolytic cell, controlled anodic electrochemical dissolution takes place with the tool as the cathode and the workpiece as the anode while applying a voltage between the workpiece and the tool [4]. An electrolyte is pumped through the small gap which is maintained between the tool and the workpiece. The chemical properties of the electrolyte are such that the constitution of the work material goes into the solution by the electrolytic process, but does not plate on the tool. With the continuation of the dissolution process, the products of the machining process are removed while circulating the electrolyte at a high velocity through the gap between the electrodes. The initial gap increases in size as metal ions remove from the anode, which increases the electrical resistance across the gap and, in turn, reduces the current flow. To maintain the initial current flow and rate of metal removal, the gap between the electrodes is maintained the same by advancing the cathode toward the anode at the same rate at which the metal is being dissolved. As the cathode tool advances during the machining operation, the anode workpiece gradually attains a shape that is almost a replica of the cathode. The ECM process generates no burrs, no stress, and has a

R. Mukherjee · S. Chakraborty (✉)
Department of Production Engineering, Jadavpur University,
Kolkata 700 032, West Bengal, India
e-mail: s_chakraborty00@yahoo.co.in

longer tool life, with damage-free machined surface, high material removal rate, and surface quality [2]. In recent years, the ECM process has also received much attention in the fabrication of micro-parts and micro-components [5].

Because of various complex physicochemical and hydrodynamic phenomena that occur in the machining gap during the course of machining, it is often very difficult to determine the optimal operating parameters of the ECM process for improved machining performance. It is observed that different ECM process parameters, such as applied voltage, machining current, electrolyte type, electrolyte concentration, electrolyte flow rate, inter-electrode gap, etc., generally influence the performance measures (responses) of the ECM process, e.g., metal removal rate, surface finish, and dimensional and profile accuracy. As different machining parameters of the ECM process have numerous and diverse ranges, suitable selection of those ECM process parameters greatly depends on the operator's technological knowledge and experience. The values for different machining parameters provided by the manufacturers cannot meet the operator's requirements. But sometimes, for achieving maximum machining performance, the optimal machining conditions are required for a particular industrial application. Hence, there is always a tremendous need for determining the optimal combination of various ECM process parameters to fulfill the requirements of the operators and also to have enhanced machining performance.

Hewidy and Fattouh [6] applied the response surface methodology (RSM) technique to study the influence of various machining parameters, such as feed rate, applied voltage, electrolyte conductivity, and electrolyte flow rate, on the width of cut, electrolyzing current, and volumetric metal removal rate of electrochemical cutting process where tubular cathodes were used. Bhattacharyya and Sorkhel [7] observed the effects of different ECM process parameters, like electrolyte concentration, electrolyte flow rate, applied voltage, and inter-electrode gap, on two machining responses, i.e., metal removal rate (MRR) and overcut (OC) phenomena, using the RSM technique. The optimal combinations of the process parameters were obtained for maximum MRR and minimum OC. Ebeid et al. [8] considered applied voltage, feed rate, back pressure, and vibration amplitude as the dominant process parameters to improve the machining accuracy in ECM while hybridizing the process by low-frequency vibrations. Using the RSM approach, the effects of those ECM process parameters on overcut and conicity were also studied to achieve high dimensional accuracy. Munda et al. [9] determined the optimal combination of pulse on/off ratio, machining voltage, electrolyte concentration, voltage frequency, and tool vibration frequency in an electrochemical micromachining process to minimize micro-spark and stray-current-affected zone in the machined

workpiece surface. Asokan et al. [10] considered current, voltage, electrolyte flow rate, and inter-electrode gap as the major ECM process parameters, and MRR and surface roughness (SR) as the two machining responses. Applying grey relational analysis, the grey grades were calculated for representing the multi-objective model. Then, multiple regression and artificial neural network (ANN) models were developed to map the relationship between the process parameters and objectives in terms of grey grades. ANN was considered as the best prediction model having less percentage deviation, and subsequently, the ECM process parameters were optimized. Munda and Bhattacharyya [11] investigated the influences of pulse on/off ratio, machining voltage, electrolyte concentration, voltage frequency, and tool vibration frequency on two predominant electrochemical micromachining (EMM) responses, i.e., MRR and radial overcut (ROC) using the RSM technique. The optimal parametric combination of those EMM process variables was also obtained for higher machining rate with accuracy. Senthilkumar et al. [12] studied the effects of applied voltage, electrolyte concentration, electrolyte flow rate, and tool feed rate on MRR and SR (i.e., R_a) for the effective electrochemical machining of LM25 Al/10%SiC composites and then optimized the process parameters using the RSM technique. Munda et al. [13] investigated the interactive and high-order influences of the pulse on/off ratio, machining voltage, electrolyte concentration, voltage pulse frequency, and micro-tool vibration frequency on ROC in the EMM process using the RSM approach. Senthilkumar et al. [14] applied non-dominated sorting genetic algorithm (NSGA-II) to optimize four ECM process parameters, e.g., electrolyte concentration, electrolyte flow rate, applied voltage, and tool feed rate, in order to maximize MRR and minimize SR (i.e., R_a). El-Taweel and Gouda [15] measured the performance of an electrochemical turning (WECT) process through studying the effects of different machining parameters, e.g., applied voltage, wire feed rate, wire diameter, workpiece rotational speed, and overlap distance on MRR, SR, and roundness error (RE). The RSM technique was then employed to search out the optimal process parameter combinations to maximize MRR and minimize SR and RE. Using the RSM approach, Haridy et al. [16] integrated the design of experiments and statistical process control to execute the experimental procedures and investigate a reliable mathematical model for optimizing the WECT process. Multi-objective optimization was performed for determining the optimal process parameter values.

Past researchers have applied several mathematical techniques, like Gauss–Jordan algorithm [7], grey relational analysis and artificial neural network [10], desirability function [9, 12, 15, 16], and non-dominated sorting genetic algorithm [14], to optimize the machining parameters of the ECM processes, but in most of the cases, suboptimal solutions have been obtained. In this paper, an attempt is

made to employ an almost unexplored optimization technique, i.e., biogeography-based optimization (BBO) algorithm, to search out the optimal combination of various machining parameters to enhance the machining performance of the ECM processes. Comparative results of its optimization performance with respect to other population-based non-conventional optimization algorithms, like genetic algorithm (GA) and artificial bee colony (ABC) algorithm, prove its universal applicability as a fast global optimization tool.

2 Biogeography-based optimization algorithm

From the early 1960s, various mathematical models were developed copying different phenomena of nature. The mindset of the engineers is that they can learn from nature. Engineers follow natural rules, such as genetic algorithm, where the laws of genetics are transformed into a mathematical model to be used as an optimization tool; in artificial neural network, the study of neurons and their functionality is involved. Similarly, the social behavior of ants and honeybees are the motivation for the emergence of ant colony optimization and ABC algorithms, respectively. Likewise, the BBO algorithm takes into consideration the mathematics of the biological distribution of different species to solve complex optimization problems [17]. As the BBO algorithm has features in common with other biology-based optimization methods, e.g., GA and ABC, it can also be applied to the same types of problems that the other biology-based optimization methods are used for, i.e., high-dimension problems with multiple local optima [18]. However, the BBO algorithm also has some features unique from the other biology-based optimization methods.

The fundamental idea behind the BBO algorithm is how species migrate from one island to another, how new species arise, and how species become extinct [19]. The term “habitat” is used to describe a geographical location that is isolated from other locations. These geographical areas are characterized by the “habitat suitability index” (HSI) and “suitability index variable” (SIV). In the BBO algorithm, each geographical location/island is considered as a “habitat” with a HSI, which is similar to the fitness function of other optimization algorithms. A good solution has a high HSI; a poor solution has a low HSI. HSI defines whether the habitat is suitable for residence or not. Habitats that are well suited as residences for biological species are said to have a high HSI. Features that correlate with HSI include factors like rainfall, diversity of vegetation, diversity of topographic features, land area, and temperature. The variables that characterize habitability are called SIVs. SIVs can be considered as the independent variables of the habitat, while HSI can be considered as the dependent variable.

Habitats with a high HSI have many species that emigrate to nearby habitats, simply by virtue of the large number of species that they host. Habitats with a high HSI have a low species immigration rate because they are already nearly saturated with species. Therefore, high-HSI habitats are more static in their species distribution than low-HSI habitats. In the same way, high-HSI habitats have a high emigration rate; the large number of species on high-HSI islands has many opportunities to emigrate to neighboring habitats. Habitats with a low HSI have a high species immigration rate because of their sparse populations. This immigration of new species to low-HSI habitats may raise the HSI of the habitat because the suitability of a habitat is proportional to its biological diversity. However, if a habitat’s HSI remains low, then the species that reside there will tend to go extinct, which will further open the way for additional immigration. Due to this, low-HSI habitats are more dynamic in their species distribution than high-HSI habitats.

Biogeography is nature’s way of distributing species and is analogous to general problem solutions. Suppose that there is a problem with some candidate solutions. The problem can be from any field of engineering and technology, provided that there is quantifiable measure of suitability of the given solution [18]. A good solution is analogous to a habitat with a high HSI, and a poor solution represents a habitat having a low HSI. High-HSI solutions resist change more than low-HSI solutions. High-HSI solutions tend to share their features with low-HSI solutions. Poor solutions accept a lot of new features from good solutions. This addition of new features to low-HSI solutions may raise the quality of the solutions. This is the central theme of the BBO algorithm.

In this algorithm, each individual has its own immigration rate (λ) and emigration rate (μ) which depend on the number of species in that habitat. The immigration rate is a monotonically non-increasing function of HSI and is proportional to the likelihood that species from neighboring habitats will migrate into a particular habitat (H_i). On the other hand, the emigration rate is a monotonically non-decreasing function of HSI and is proportional to the likelihood that species from H_i habitat will migrate into the neighboring habitats. Usually, it is assumed that both λ and μ are linear with the same maximum values. However, these assumptions are made only for mathematical convenience, and better performance might be attainable if these assumptions are relaxed [20–23]. In the immigration curve [19], the maximum possible immigration rate to the habitat is I , which occurs when there are zero species in the habitat. As the number of species increases, the habitat becomes more crowded, fewer species are able to successfully survive immigration to the habitat, and the immigration rate gradually decreases. The largest possible number of species that the habitat can support is S_{max} , at which point the immigration rate becomes zero. On the other hand, if there

are no species in the habitat, then the emigration rate must be zero. As the number of species increases, the habitat becomes more crowded, more species are able to leave the habitat to explore other possible residences, and the emigration rate increases. The maximum emigration rate is E , which occurs when the habitat contains the largest number of species that it can support. The equilibrium number of species is S_0 , at which point the immigration and emigration rates are equal. However, there may be occasional excursions due to temporal effects. Positive excursions could be due to a sudden spurt of immigration or a sudden burst of speciation. Negative excursions could be due to disease, the introduction of an especially ravenous predator, or some other natural catastrophe. The emigration and immigration rates of each solution are used to probabilistically share information between habitats. With probability P_{mod} , each solution is modified based on other solutions. If a given solution is selected to be modified, then its immigration rate is used to probabilistically decide whether or not to modify each SIV in that solution. If a given SIV (S_i) in a given solution is selected to be modified, then the emigration rates of the other solutions are used to probabilistically decide which of the solutions should migrate a randomly selected SIV to solution S_i .

The BBO algorithm is presented as below [19]:

1. Initialize the BBO parameters, like habitat modification probability, mutation probability, maximum species count (n), maximum migration rates E and I , maximum mutation rate (m_{max}), elitism parameter, and number of habitats (NP)
2. Initialize the generation counter ($g=0$).
3. Create a random population, $\vec{X}_{i,g}$ ($i=1,2,\dots,\text{NP}$).
4. Evaluate $f(\vec{X}_{i,g})$.
5. **for** $g=1$ to MAX_{GEN} **do**
6. **for** $i=1$ to NP **do**
7. Sort the population from the best fit to the least fit.
8. Map the HSI to the number of species.
9. Calculate the immigration rate (λ_i) and the emigration rate (μ_i).
10. Modify the non-elite members of population probabilistically with the migration operator.
11. **end for**
12. **for** $i=1$ to NP **do**
13. Mutate the non-elite members of population probabilistically with the mutation operator.
14. **end for**
15. **for** $i=1$ to NP **do**
16. Evaluate the new individuals in the population.
17. Replace the habitats with their new versions.
18. Replace the worst with the previous generation's elites.
19. **end for**
20. $g=g+1$
21. **end for**

In this algorithm, mutation is used to enhance the diversity of the population that helps decrease the chances of getting the local minima [21]. For low-HSI solutions, mutation gives them a chance of enhancing the quality of solutions, and for high-HSI solutions, mutation is able to improve them even more than they already have. On the other hand, elitism (copying some of the fittest individuals to the next generation) is applied to guarantee that the fitness function increases monotonically with successive generations. This prevents the best solutions from being corrupted by immigration. The migration operator is used to share information between solutions.

3 Optimization of electrochemical machining processes

In order to validate the applicability and performance of the BBO algorithm for parametric optimization, the experimental data and mathematical modeling of an ECM process [7] and a WECT process [15] are considered here. For each of the processes, both the single- and multi-objective optimizations of the responses are performed. For parametric optimization of the ECM processes, the related computer code for the BBO algorithm is developed in MATLAB 7.6 (R2008a) with the following control parameters [17].

Habitat modification probability	1
Mutation probability	0.005
Maximum species count	500
Maximum immigration rate	1
Maximum emigration rate	1
Maximum mutation rate	0
Elitism parameter	2
Generation count limit	50
Number of genes in each population member	20

3.1 Example 1

In a developed microprocessor-based auto-tool-feed ECM setup, Bhattacharyya and Sorkhel [7] conducted experiments on cylindrical workpieces (19 mm in diameter made

Table 1 Machining parameters with their levels for ECM process [7]

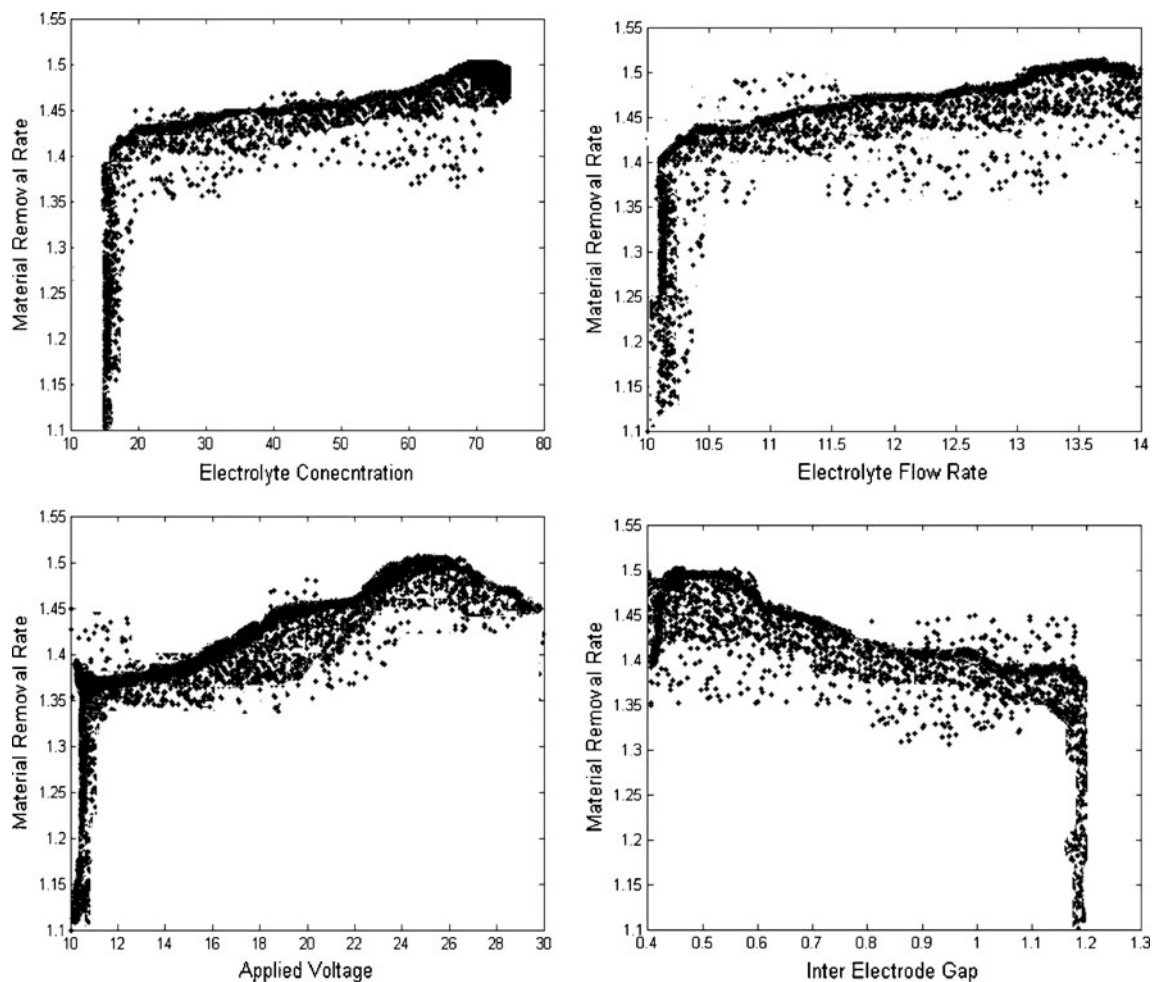
Parameters	Levels				
	-2	-1	0	1	2
Electrolyte concentration (g/l)	15	30	45	60	75
Electrolyte flow rate (l/min)	10	11	12	13	14
Applied voltage (V)	10	15	20	25	30
Inter-electrode gap (mm)	0.4	0.6	0.8	1	1.2

Table 2 Single-objective optimization results for ECM process

Optimization method	Response	Value	Electrolyte concentration (g/l)	Electrolyte flow rate (l/min)	Applied voltage (V)	Inter-electrode gap (mm)
Bhattacharyya and Sorkhel [7]	MRR	0.8230	57.88	11.98	22.04	0.001
	OC	0.2706	17.55	11.05	21.65	0.870
GA	MRR	1.1603	64.56	10.40	29.48	0.778
	OC	0.2369	28.65	12.40	13.56	0.530
ABC algorithm	MRR	1.3077	60.28	13.65	24.77	0.424
	OC	0.2067	26.85	13.66	11.75	0.602
BBO algorithm	MRR	1.5069	67.60	13.80	26.90	0.440
	OC	0.1320	15.85	10.25	12.45	0.500

of EN-8 steel) using cylindrical solid brass tools (16 mm in diameter). Sodium chloride (NaCl) salt solution was selected as the electrolyte because of its high conductivity and non-passive characteristics. Four machining parameters, i.e., electrolyte concentration, electrolyte flow rate, applied voltage, and inter-electrode gap, and two process performances (responses), i.e., MRR (in gm/min) and OC (in millimeters)

were considered. MRR can be defined as the amount of material removed from the workpiece surface in unit machining time, whereas OC is the difference between the size of the electrode and the size of the cavity created during the machining operation. Each of the four machining parameters was set at five different levels, as shown in Table 1. A central composite rotatable second-order experimentation plan was

**Fig. 1** Variations of MRR with respect to ECM process parameters

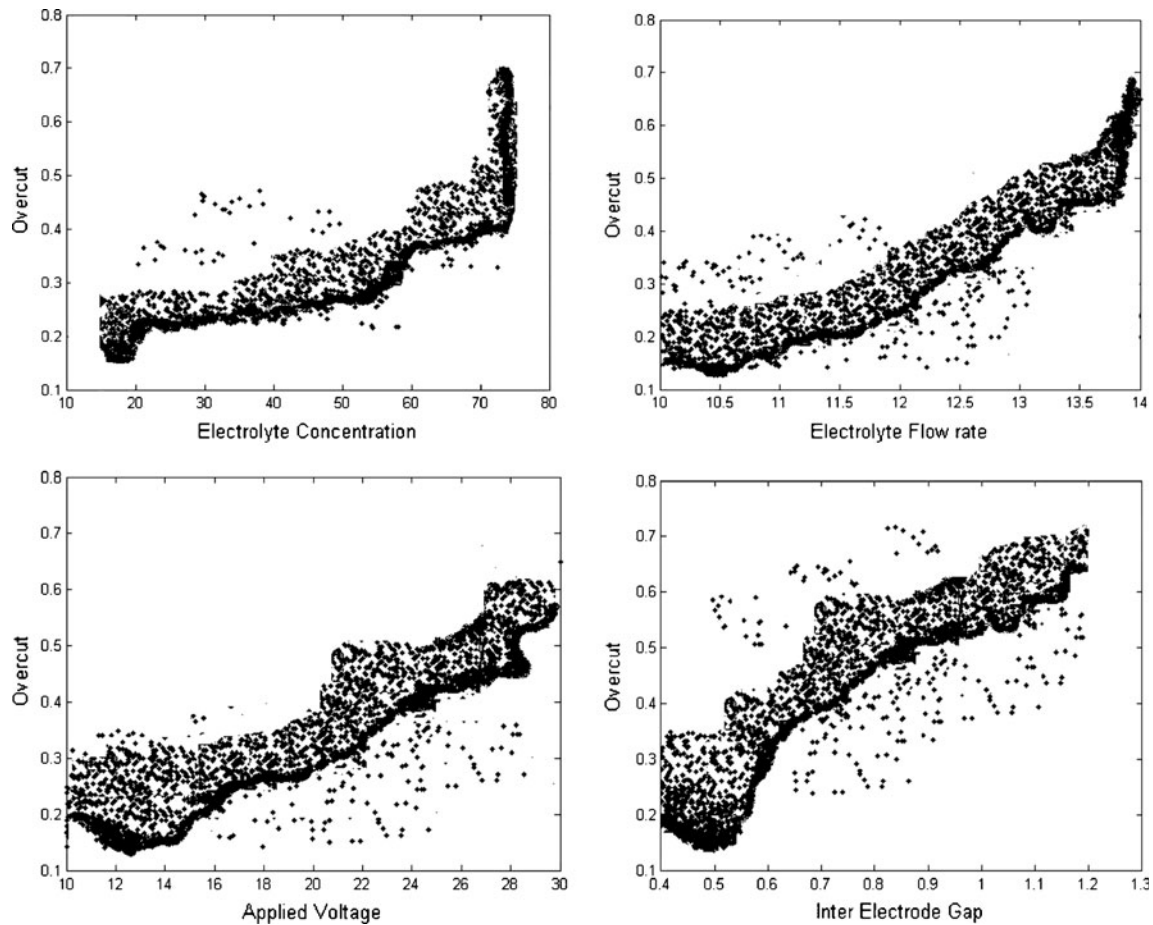


Fig. 2 Variations of OC with respect to ECM process parameters

used with 31 experimental runs, and then the RSM technique was employed to develop two second-order polynomial regression equations (including interaction effects) for the responses. These RSM-based equations are given as below.

$$\begin{aligned}
 Y_u(\text{MRR}) = & 0.6244 + 0.1523x_1 + 0.0404x_2 + 0.1519x_3 \\
 & - 0.1169x_4 + 0.0016x_1^2 + 0.0227x_2^2 + 0.0176x_3^2 \\
 & - 0.0041x_4^2 + 0.0077x_1x_2 + 0.0119x_1x_3 \\
 & - 0.0203x_1x_4 + 0.0103x_2x_3 - 0.0095x_2x_4 \\
 & + 0.0300x_3x_4
 \end{aligned} \quad (1)$$

$$\begin{aligned}
 Y_u(\text{OC}) = & 0.3228 + 0.0214x_1 - 0.0052x_2 + 0.0164x_2 \\
 & + 0.0118x_4 - 0.0041x_1^2 - 0.0122x_2^2 + 0.00274x_3^2 \\
 & + 0.0034x_4^2 - 0.0059x_1x_2 - 0.0046x_1x_3 \\
 & - 0.0059x_1x_4 + 0.0021x_2x_3 - 0.0053x_2x_4 \\
 & - 0.0078x_3x_4
 \end{aligned} \quad (2)$$

where x_1 is the electrolyte concentration, x_2 is the electrolyte flow rate, x_3 the applied voltage, and x_4 the inter-electrode gap.

3.1.1 Single-objective optimization

The BBO algorithm is now applied to optimize the two RSM-based equations with respect to the constraints as imposed by the chosen limiting values of the four ECM process parameters, i.e., $15 \leq x_1 \leq 75$, $10 \leq x_2 \leq 14$, $10 \leq x_3 \leq 30$, and $0.4 \leq x_4 \leq 1.2$. Here, the responses are separately optimized. Between these two responses, MRR is to be maximized and OC is to be minimized. For any machining process, it is always desirable

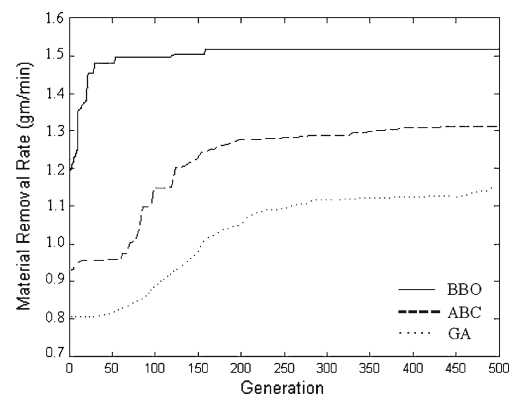


Fig. 3 Convergence of GA and the BBO and ABC algorithms for MRR

Table 3 Computation times for the three algorithms

Optimization method	Average CPU time (s)
GA	21.5
ABC algorithm	22.0
BBO algorithm	20.5

to remove as much material as possible from the workpiece surface within a given machining time; on the other hand, as OC is a dimensional deviation, it is preferred to minimize that deviation in order to obtain an almost accurate machined component. Bhattacharya and Sorkhel [7] also solved these RSM-based equations using Gauss–Jordan algorithm and obtained the optimal settings of the ECM process parameters, as shown in Table 2. This table also exhibits the optimal ECM process parameter settings and response values as achieved using the BBO algorithm. The MRR is drastically increased from 0.8230 to 1.5069 g/min and OC is significantly reduced from 0.2706 to 0.1320 mm. The optimal ECM process settings are also changed. The optimal results obtained from the BBO algorithm are also compared with those derived by GA and the ABC algorithm, as given in Table 2. It is revealed that the BBO algorithm clearly outperforms the other two population-based optimization algorithms.

Bhattacharya and Sorkhel [7] extensively studied the effects of four ECM process parameters on MRR and OC and observed that for maximum MRR, an increase in electrolyte concentration, an increase in electrolyte flow rate, an increase in applied voltage, and a decrease in the inter-electrode gap would be the requirements. On the other hand, a decrease in electrolyte concentration, a decrease in the electrolyte flow rate, a decrease in applied voltage, and a decrease in the inter-electrode gap would give a minimum OC value. These same findings are also observed in Figs. 1 and 2 where the variations of MRR and OC are respectively shown with respect to the considered ECM process parameters. Thus, a combination of electrolyte concentration=67.60 g/l, electrolyte flow rate=13.80 l/min, applied voltage=26.90 V, and inter-electrode gap=0.440 mm would maximize the MRR (1.5069 g/min). On the other hand, the minimum value of OC (0.1320 mm) would be obtained at a combination of

electrolyte concentration=15.85 g/l, electrolyte flow rate=10.25 l/min, applied voltage=12.45 V, and inter-electrode gap=0.500 mm. It can be observed that for the two responses, the optimal ECM process parameter settings are different, which would be impossible to maintain when both the responses are required to be simultaneously optimized.

The performance of the BBO algorithm with respect to computation speed (convergence) is shown in Fig. 3 along with GA and the ABC algorithm when all these optimization algorithms are run in an Intel Core 2 DUO, 1.83-GHz, 0.99-GB RAM CPU computer platform. For the GA, various control parameters are set as crossover type=1, crossover probability=0.95, initial mutation probability=0.01, generation count limit=50, and maximum species count=500. On the other hand, the control parameters for the ABC algorithm are fixed as colony size=10, maximum cycle number=500, limit control parameter to abandon the food source=100, run time=3, and maximum species count=500. Table 3 portrays a comparison between the computation (CPU) time requirements for these three algorithms. It is worthwhile to note that for single-objective optimization, the CPU times for these algorithms are not at all widely different and that the BBO algorithm has slight superiority over the others. As Bhattacharya and Sorkhel [7] considered Gauss–Jordan algorithm (an iterative-based optimization technique), its convergence performance cannot be compared with that of the BBO algorithm.

3.1.2 Multi-objective optimization

In multi-objective optimization of the ECM process, instead of treating the two responses separately, both are simultaneously optimized. For this, the following objective function is developed [24].

$$\text{Min}(Z_1) = w_1 Y_u(\text{OC})/\text{OC}_{\min} - w_2 Y_u(\text{MRR})/\text{MRR}_{\max} \quad (3)$$

where $Y_u(\text{OC})$ and $Y_u(\text{MRR})$ are the second-order response surface equations for OC and MRR, respectively; OC_{\min} and MRR_{\max} are the minimum and maximum values of OC and MRR, respectively; and w_1 and w_2 are the weight values assigned to OC and MRR, respectively. The minimum and maximum values of OC and MRR are obtained from the single-objective optimization results. The weight values can

Table 4 Multi-objective optimization using the BBO algorithm

Case	Response	Value	Z_1	Electrolyte concentration (g/l)	Electrolyte flow rate (l/min)	Applied voltage (V)	Inter-electrode gap (mm)
Case 1 ($w_1=0.5, w_2=0.5$)	MRR	1.3230	-0.5108	67.05	13.90	20.07	0.434
	OC	0.2290					
Case 2 ($w_1=0.9, w_2=0.1$)	MRR	0.8186	0.1416	49.95	13.69	12.31	0.544
	OC	0.1896					
Case 3 ($w_1=0.1, w_2=0.9$)	MRR	1.4489	-1.2335	72.15	13.93	27.10	0.706
	OC	0.2346					

Table 5 Machining parameters with their levels for the WECT process [15]

Parameters	Levels				
	-2	-1	0	1	2
Applied voltage, U (V)	10	17.5	25	32.5	40
Wire feed rate, f (mm/min)	0.1	0.2	0.3	0.4	0.5
Wire diameter, d (mm)	0.2	0.65	1.1	1.55	2
Overlap distance, h (mm)	0.02	0.03	0.04	0.05	0.06
Workpiece rotational speed, N (rpm)	300	450	600	750	900

be anything provided that $w_1 + w_2 = 1$, and it depends on the priorities of the considered responses as set by the process engineers. Here, equal weights for both the responses, i.e., $w_1 = w_2 = 0.5$ (case 1) are first considered; the results obtained after solving this multi-objective optimization problem using the BBO algorithm are given in Table 4. The MRR and OC values are obtained as 1.3230 g/min and 0.2290 mm, respectively, and the optimal solution (Z_j) is -0.5108 . Bhattacharya and Sorkhel [7] did not consider the problem of multi-objective optimization of the responses; hence, the results of Table 4 cannot be compared here. However, these results are far better than those obtained by Bhattacharya and Sorkhel [7] while treating the responses separately. Table 4 also shows the results of multi-response optimization when two other cases having unequal weights to the responses are considered (case 2: $w_1 = 0.9$, $w_2 = 0.1$; case 3: $w_1 = 0.1$, $w_2 = 0.9$). In both these cases, different optimal ECM process parameter settings are observed. Depending upon the requirements, the process engineers can select any of these weight schemes to the responses and correspondingly choose the optimal process parameter values to achieve the desired results.

3.2 Example 2

El-Taweel and Gouda [15] considered five controllable machining parameters, i.e., wire diameter, wire feed rate, applied voltage, workpiece rotational speed, and overlap distance, and three responses, i.e., MRR (in gm/min), SR (R_a , in

micrometers), and RE (in micrometers) while conducting experiments in a WECT process. Each of the machining parameters was set at five different levels, as exhibited in Table 5. Experiments were performed according to a central composite second-order rotatable design plan, and three RSM-based second-order equations were subsequently developed for the considered responses. In the RSM-based equations for SR (R_a) and RE, as developed by El-Taweel and Gouda [15], one unknown variable (V) was wrongly introduced, which might be due to some typing mistake. Hence, using the experimental plan and data of El-Taweel and Gouda [15], three RSM equations are again developed applying Design Expert (version 8.0.4) software. These three new equations are shown below:

$$\begin{aligned} \text{MRR} = & 0.21 + 0.051x_1 + 0.017x_2 + 6.167 \times 10^{-3}x_3 \\ & + 4.667 \times 10^{-3}x_4 + 0.011x_5 - 5 \times 10^{-4}x_1x_2 \\ & + 4.375 \times 10^{-3}x_1x_3 - 0.011x_1x_4 + 4.375 \times 10^{-3}x_1x_5 \\ & + 0.014x_2x_3 + 7.625 \times 10^{-3}x_2x_4 + 0.012x_2x_5 \\ & - 2 \times 10^{-3}x_3x_4 + 0.014x_4x_5 + 2.068 \times 10^{-3}x_1^2 \\ & - 5.557 \times 10^{-3}x_2^2 - 0.21x_3^2 - 4.057 \times 10^{-3}x_4^2 \\ & + 4.068 \times 10^{-3}x_5^2 \end{aligned} \quad (4)$$

$$\begin{aligned} R_a = & 1.68 + 0.17x_1 + 0.067x_2 - 0.21x_3 + 0.12x_4 - 0.14x_5 \\ & + 0.11x_1x_2 + 0.024x_1x_3 + 0.28x_1x_4 + 0.033x_1x_5 \\ & + 0.031x_2x_3 + 0.086x_2x_4 - 0.011x_2x_5 + 0.048x_3x_4 \\ & + 0.15x_3x_5 + 0.018x_4x_5 - 0.026x_1^2 - 0.019x_2^2 - 0.019x_3^2 \\ & - 0.019x_4^2 - 0.032x_5^2 \end{aligned} \quad (5)$$

Table 6 Single-objective optimization results for the WECT process

Optimization method	Response	Value	Applied voltage	Wire feed rate	Wire diameter	Overlap distance	Workpiece rotational speed
GA	MRR	0.2356	27.30	0.4390	1.3758	0.0223	892.50
	R_a	0.7656	10.22	0.2500	1.4600	0.0450	825
	RE	6.7153	31.35	0.4100	0.5600	0.0300	638.40
ABC algorithm	MRR	0.3126	17.45	0.1380	1.7600	0.0346	898
	R_a	0.4269	14.65	0.4390	0.3620	0.0330	892.50
	RE	4.5165	34.30	0.4750	1.2670	0.0492	813
BBO algorithm	MRR	0.4068	35.15	0.4730	1.0775	0.0571	886.75
	R_a	0.1081	11.50	0.1230	1.7570	0.0539	512.76
	RE	2.7764	21.35	0.4590	0.8930	0.0360	759

$$\begin{aligned}
 RE = & 7.21 + 1.99x_1 - 1.31x_2 + 1.71x_3 - 1.09x_4 - 2.39x_5 \\
 & - 0.17x_1x_2 - 0.32x_1x_3 + 0.033x_1x_4 - 1.18x_1x_5 - 0.41x_2x_3 \\
 & + 0.4x_2x_4 - 5 \times 10^{-3}x_2x_5 - 0.068x_3x_4 - 0.62x_3x_5 + 0.91x_4x_5 \\
 & + 0.5x_1^2 + 0.021x_2^2 + 0.19x_3^2 + 0.28x_4^2 + 0.56x_5^2
 \end{aligned}
 \tag{6}$$

where x_1 is the applied voltage, x_2 the wire feed rate, x_3 the wire diameter, x_4 the overlap distance, and x_5 is the work-piece rotational speed.

3.2.1 Single-objective optimization

In their research outcomes, El-Taweel and Gouda [15] did not perform single-objective optimization of any of the considered responses. Table 6 shows the results of the single-objective optimization of the responses when the BBO algorithm is employed to solve the three RSM-based equations, as given in Eqs. 4, 5, and 6. The constraints for these optimization

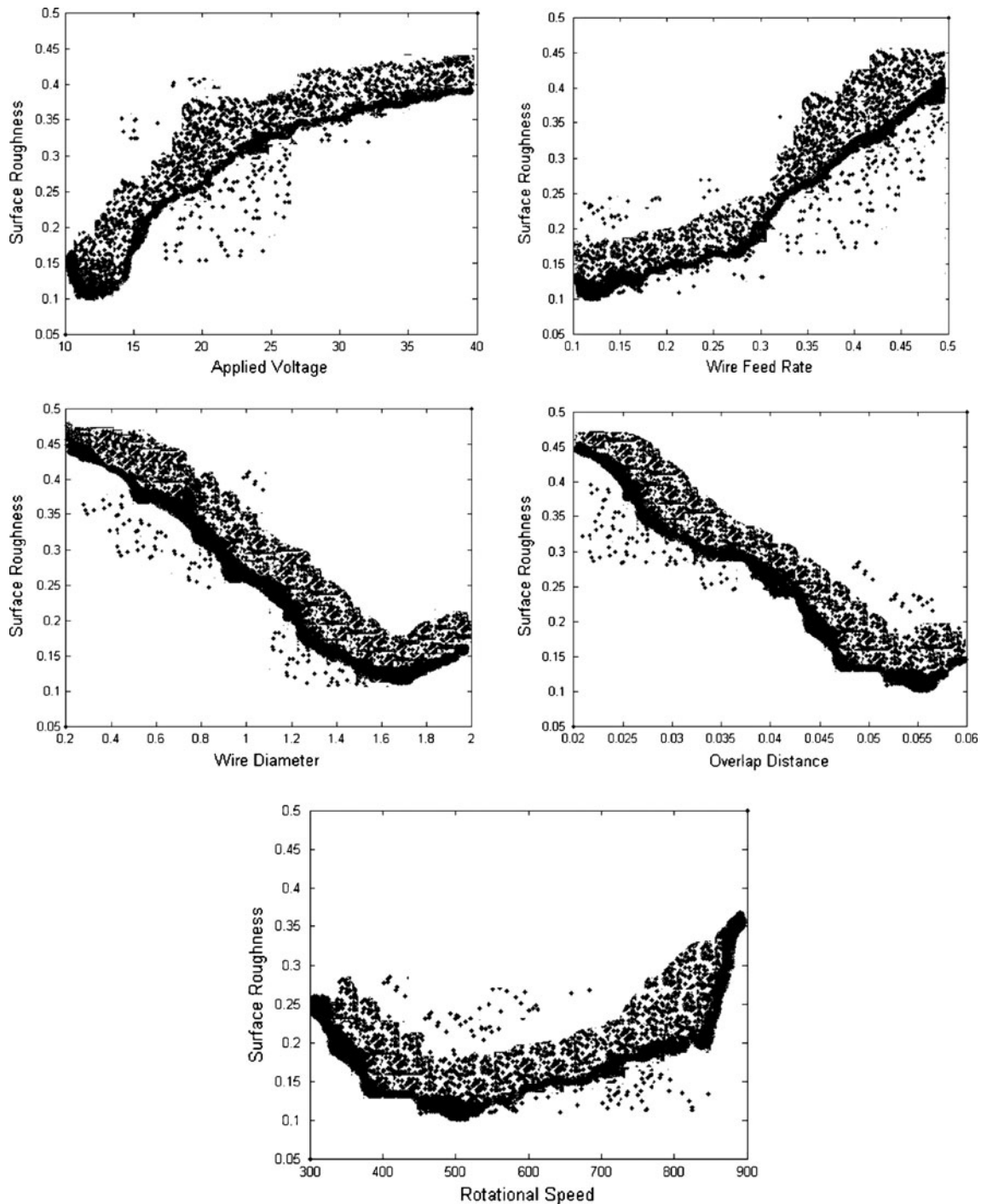


Fig. 4 Variations of surface roughness with respect to WCET process parameters

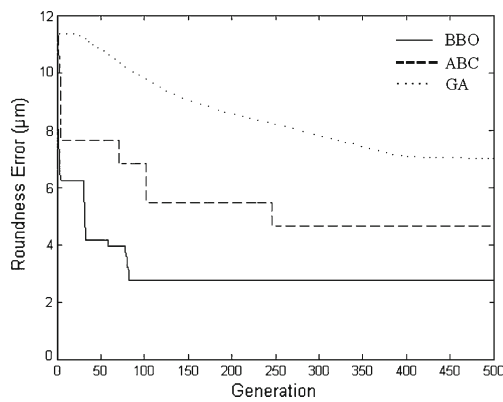


Fig. 5 Convergence of GA and the BBO and ABC algorithms for RE

problems are set based on the range of the five WECT process parameter values, as given in Table 5, i.e., $10 \leq x_1 \leq 40$, $0.1 \leq x_2 \leq 0.5$, $0.2 \leq x_3 \leq 2$, $0.02 \leq x_4 \leq 0.06$, and $300 \leq x_5 \leq 900$. Table 6 also compares the solutions when GA and the ABC algorithm are applied for the same three single-objective optimization problems. While solving these single-objective optimization problems for the considered three responses, GA and the ABC and BBO algorithms take average computation times of 25.33, 24.67, and 24.33 s, respectively. At the optimal WECT process parameter combination, as derived using the BBO algorithm, the MRR is drastically improved and the R_a and RE values are significantly reduced. It proves the superiority of the BBO algorithm over the other two optimization algorithms.

Figure 4 displays the variations of surface roughness with respect to the five WECT process parameters. From this figure, it is observed that with the increment of the applied voltage and wire feed rate, the surface roughness increases. On the other hand, an almost decreased value of surface roughness is achieved when the wire diameter and overlap distance are increased. In the case of workpiece rotational speed, with its increased value, the surface roughness gradually decreases and then, reaching its minimum, the surface roughness starts increasing. These findings totally corroborate with those observed by El-Taweel and Gouda [15]. It has been observed that with the increase in applied voltage, there is an accumulation of machining sludge in the inter-electrode gap which increases the tendency of sparking. This entire process mechanism plays a vital role in enhancing the surface roughness. It

has also been found out that with increasing wire diameter, the surface roughness is greatly improved. Increased wire diameter leads to an increase in the workpiece surface area exposed to machining, which, in turn, improves the surface roughness. It has been noted that the surface roughness increases with increased wire feed rate, which may be due to the spiral path of the wire along the workpiece in the WECT process. This spiral path of the wire is generated because of the wire feed rate and rotation of the workpiece. The pitch of the spiral path increases while increasing the feed rate and thus produces a rough surface. With the increase in workpiece rotational speed, the surface roughness decreases initially, which is due to the improvement of the electrolyte flow around the workpiece, increased current density in the machining gap, and good flushing of the machined products, resulting in a decrease in the tendency of sparking. After reaching its minimum value, the surface roughness increases with the increase in the workpiece rotational speed, which may be due to the high turbulence created in the machining zone.

The variations of the other two responses, i.e., MRR and RE, with respect to the WECT process parameters are also studied, and the observations are almost the same as those obtained by El-Taweel and Gouda [15]. These are not shown here due to lack of space. Figure 5 exhibits the convergence of the GA and the BBO and ABC algorithms with respect to RE.

3.2.2 Multi-objective optimization

For multi-objective optimization of WECT process, El-Taweel and Gouda [15] applied the desirability function approach and obtained values of MRR as 0.298029 g/min, R_a as 1.12941 μm , and RE as 5.54323 μm at the optimal parametric combination. These results are shown in Table 7. Now, the BBO algorithm is employed for this multi-objective optimization problem, considering equal weights for all the three responses. The objective function for this multi-objective optimization is given below:

$$\begin{aligned} \text{Min}(Z_2) = & 0.3333 \times R_a/R_{a\min} + 0.3333 \times \text{RE}/\text{RE}_{\min} \\ & - 0.3333 \times \text{MRR}/\text{MRR}_{\max} \end{aligned} \quad (7)$$

where $R_{a\min}$, RE_{\min} , and MRR_{\max} are the minimum, minimum, and maximum values of R_a , RE, and MRR, respectively, which

Table 7 Results of multi-objective optimization for the WECT process

Optimization method	Response	Value	Applied voltage	Wire feed rate	Wire diameter	Overlap distance	Workpiece rotational speed
El-Taweel and Gouda [15]	MRR	0.298029	32.499	0.4	1.312	0.03	750
	R_a	1.12941					
	RE	5.54323					
BBO algorithm	MRR	0.3545	36.43	0.438	1.25	0.0299	894
	R_a	0.8303					
	RE	2.0456					

are derived from the single-objective optimization results. It is observed from the results of the BBO algorithm, as given Table 7, that at the optimal settings of applied voltage=36.43 V, wire feed rate=0.438 mm/min, wire diameter=1.25 mm, overlap distance=0.0299 mm, and workpiece rotational speed=894 rpm, the MRR is increased to 0.3545 g/min, R_a is reduced to 0.8303 μm , and RE is also decreased to 2.0456 μm . The objective function value (Z_2) is calculated as 0.8283, and its positive value indicates that the combined effect of R_a and RE is more than that of MRR. These results prove that the BBO algorithm is far better than the desirability function approach, as adopted by El-Taweel and Gouda [15].

4 Conclusions

In this paper, the biogeography-based optimization algorithm is applied to search out the best combinations of operating parameters for electrochemical machining and wire electrochemical turning processes for achieving better machining performance. This algorithm is used to solve both the single- and multi-objective optimization problems. When compared with other population-based optimization algorithms, it is observed that the BBO algorithm outperforms them in terms of solution accuracy and computation speed. Thus, the BBO algorithm proves its applicability and universal acceptability as a global optimization tool for selection of the process parameter values. It can also be successfully applied to optimize the operating parameters of other non-traditional machining processes, like electric discharge machining, wire electric discharge machining, laser beam machining, ultrasonic machining, and plasma arc machining processes. Not entirely depending on the manufacturer's data, the process engineers can now set the optimal values of various operating parameters for different processes to achieve the best machining performance.

References

- McGeough JA (1974) Principles of electrochemical machining. Chapman Hall, London
- Jain VK (2005) Advanced machining processes. Allied Publishers, New Delhi
- Pandey PC, Shan HS (2005) Modern machining processes. Tata McGraw-Hill, New Delhi
- Bhattacharyya B (2010) Electrochemical micromachining. In: Jain VK (ed) Introduction to micromachining. Narosa Publishing, New Delhi 3.1–3.4
- Bhattacharyya B, Mitra S, Boro AK (2002) Electrochemical machining: new possibilities for micromachining. Robotics and Computer Integrated Manufacturing 18:283–289
- Hewidy MS, Fattouh M (1989) Electrochemical cutting using tubular cathodes: response surface approach. Int J Prod Res 27:953–963
- Bhattacharyya B, Sorkhel SK (1999) Investigation for controlled electrochemical machining through response surface methodology-based approach. J Mater Process Technol 86:200–207
- Ebeid SJ, Hewidy MS, El-Taweel TA, Youssef AH (2004) Towards higher accuracy for ECM hybridized with low-frequency vibrations using the response surface methodology. J Mater Process Technol 149:432–438
- Munda J, Malapati M, Bhattacharyya B (2007) Control of micro-spark and stray-current effect during EMM process. J Mater Process Technol 194:151–158
- Asokan P, Ravi Kumar R, Jeyapaul R, Santhi M (2008) Development of multi-objective optimization models for electrochemical machining process. Int J Adv Manuf Tech 39:55–63
- Munda J, Bhattacharyya B (2008) Investigation into electrochemical micromachining (EMM) through response surface methodology based approach. Int J Adv Manuf Tech 35:821–832
- Senthilkumar C, Ganesan G, Karthikeyan R (2009) Study of electrochemical machining characteristics of Al/SiC_p composites. Int J Adv Manuf Tech 43:256–263
- Munda J, Malapati M, Bhattacharyya B (2010) Investigation into the influence of electrochemical micromachining (EMM) parameters on radial overcut through RSM-based approach. Int J Manuf Tech Manag 21:54–66
- Senthilkumar C, Ganesan G, Karthikeyan R (2010) Bi-performance optimization of electrochemical machining characteristics of Al/20% SiC_p composites using NSGA-II. Proc IMechE J Engg Manuf 224:1399–1407
- El-Taweel TA, Gouda SA (2011) Performance analysis of wire electrochemical turning process—RSM approach. Int J Adv Manuf Tech 53:181–190
- Haridy S, Gouda SA, Wu Z (2011) An integrated framework of statistical process control and design of experiments for optimizing wire electrochemical turning process. Int J Adv Manuf Tech 53:191–207
- Simon D (2008) Biogeography-based optimization. IEEE Trans Evol Comput 12:702–713
- Simon D, Rarick R, Ergezer M, Du D (2011) Analytical and numerical comparisons of biogeography-based optimization and genetic algorithms. Inform Sci 181:1224–1248
- Boussaid I, Chatterjee A, Siarry P, Ahmed-Nacer M (2011) Two-stage update biogeography-based optimization using differential evolution algorithm (DBBO). Comp Oper Res 38:1188–1198
- Ma H (2010) An analysis of the equilibrium of migration models for biogeography-based optimization. Inform Sci 180:3444–3464
- Gong W, Cai Z, Ling CX, Li H (2010) A real-coded biogeography-based optimization with mutation. Appl Math Comput 216:2749–2758
- Ma H, Simon D (2011) Blended biogeography-based optimization for constrained optimization. Eng Appl Artif Intell 24:517–525
- Gong W, Cai Z, Ling CX (2010) DE/BBO: a hybrid differential evolution with biogeography-based optimization for global numerical optimization. Soft Computing 15:645–665
- Rao RV, Pawar PJ, Shankar R (2008) Multi-objective optimization of electrochemical machining process parameters using a particle swarm optimization algorithm. Proc IMechE J Engg Manuf 222:949–958